Dalton Transactions

# Conformational Twisting of a Formate-Bridged Diiridium Complex Enables Catalytic Formic Acid Dehydrogenation



| | |
|---|---|
| Journal: | *Dalton Transactions* |
| Manuscript ID | DT-ART-08-2018-003268.R1 |
| Article Type: | Paper |
| Date Submitted by the Author: | 01-Sep-2018 |
| Complete List of Authors: | Lauridsen, Paul; University of Southern California, Loker Hydrocarbon Research Institute<br>Lu, Zhiyao; University of Southern California, Chemistry;<br>Celaje, Jeff; University of Southern California, Loker Hydrocarbon Research Institute<br>Kedzie, Elyse; University of Southern California, Loker Hydrocarbon Research Institute<br>Williams, Travis; University of Southern California, Loker Hydrocarbon Research Institute |
| | |

Journal Name

ARTICLE

# Conformational Twisting of a Formate-Bridged Diiridium Complex Enables Catalytic Formic Acid Dehydrogenation

Paul J. Lauridsen, Zhiyao Lu, Jeff J. A. Celaje, Elyse A. Kedzie, Travis J. Williams*

Received 00th January 20xx,
Accepted 00th January 20xx

DOI: 10.1039/x0xx00000x

www.rsc.org/

We previously reported that iridium complex **1a** enables the first homogeneous catalytic dehydrogenation of neat formic acid and enjoys unusual stability through millions of turnovers. Binuclear iridium hydride species **5a**, which features a provocative C2-symmetric geometry, was isolated from the reaction as a catalyst resting state. By synthesizing and carefully examining the catalytic initiation of a series of analogues to **1a**, we establish here a strong correlation between the formation of C2-twisted iridium dimers analogous to **5a** and the reactivity of formic acid dehydrogenation: an efficient C2 twist appears unique to **1a** and essential to catalytic reactivity.

## Introduction

Formic acid (FA) is a promising hydrogen carrier, because it is a solar fuel and it enables on-demand $H_2$ release under mild conditions with $CO_2$ as the only by-product.[1,2] Ongoing research on FA dehydrogenation has identified many outstanding catalytic systems, both heterogeneous[3–8] and homogeneous.[9–13] Our group is interested in catalytic hydride manipulation,[14–19] and we have recently reported the first homogeneous iridium catalytic system for the dehydrogenation of neat FA,[20] which presents a unique challenge due to the corrosive nature of the neat liquid. Catalytic systems based on iridium complex **1a** have shown a useful average turnover frequency (TOF ca. 0.83 $s^{-1}$) through greater than 2 million turnovers under mild conditions (Scheme 1).[20] When compared to other homogeneous systems, we observe several unique advantages of ours: 1) it is highly reactive with low loading of catalyst and base; 2) it works in neat, technical-grade FA; 3) the selectivity against CO is nearly absolute (< 10 ppm).

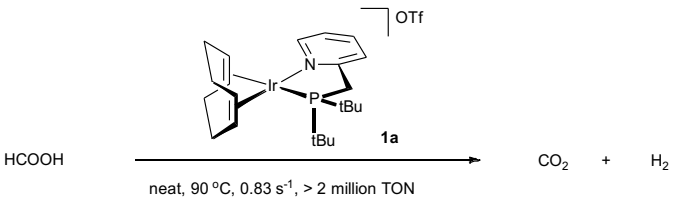


**Scheme 1**. Iridium precatalyst **1a** shows FA dehydrogenation reactivity.

Synthetic studies of the initiation sequence for our catalyst enabled us to identify several species present in the conversion of **1a**[21] to our active catalyst (Scheme 2). The sequence features three intermediates that are observable under the reactive conditions. The first is an (allyl)iridium hydride (**2a**).[19,21,22] The second is a Cs-symmetric hydride-bridged dimer (**4a**) that is analogous to many related structures characterized by Pfaltz.[23] In the presence of carboxylic acids, we find that **4a** converts easily and selectively to structurally-novel iridium complex **5a**, a binuclear, formate-bridged iridium species that is present at the beginning and end of our catalytic reaction. The acetate homologue of **5a** (**5a'**) was characterized crystallographically.[21] With the aid of distinctive hydride peaks in NMR, we showed that **5a** and its formate addition adduct, **6a**, are resting states of the catalytic reaction. Whereas **4a** is unstable to our FA dehydrogenation conditions—it converts rapidly to **5a**—we could not test directly whether the twisting of **4a** to **5a** is essential to our mechanism or simply an unavoidable thermodynamically-driven outcome.

The **5a**-catalyzed dehydrogenation of FA stands out in the FA literature, because many recent mechanistic studies show that homogeneous, iridium-catalyzed FA dehydrogenation systems rely on mononuclear catalysts,[24–26] while ours is dimeric. This presages a central question of what, if any, role the second iridium plays in the reactivity. Curiously, no other C2-twisted complexes with the iridium hydride topology of **5a** are known, although several binuclear iridium hydride complexes that structurally resemble **4a** have been synthesized,[23,27,28] and binuclear iridium complexes such as these are not well known for catalytic dehydrogenation.[23,29–32] Herein, we show that the C2 twisting behavior seen in the conversion of **4a** to **5a** is highly specific to the parent **4a**/**5a** system and that closely-related structural analogs do not participate in this transformation efficiently (or at all). We further illustrate that this twisted bimetallic structure is essential to the system's remarkable reactivity.

*Loker Hydrocarbon Research Institute and Department of Chemistry, University of Southern California, 837 Bloom Walk, Los Angeles, CA 90089-1661, USA. E-mail: travisw@usc.edu;*
*Fax: +1 213 740 5961; Tel: +1 213 740 5961*
Electronic Supplementary Information (ESI) available: preparative details, graphical spectral data, and raw kinetics data. See DOI: 10.1039/x0xx00000x

## Results and Discussion

### 1. A proposed mechanism

Scheme 2 illustrates our working mechanistic model for initiation of our FA dehydrogenation catalyst, **1a**.[19,20,22] Precatalyst **1a**[21] is first transformed to **4a** through the intermediacy of several species, including (allyl)iridium hydride complex **2a**,[21] that are not observed under catalytic conditions. Iridium dimer **4a** is one of a family of iridium species of the same iridium hydride topology that are known to occur in iridium-catalyzed hydrogenations.[23] In our hands, **4a** is stable at ambient temperature, and we have observed it directly. While we see that **4a** converts completely and rapidly to **5a** under catalytic conditions, we have not found conditions for the reverse reaction. In a formic acid/formate buffer, **5a** and **6a** are in equilibrium, and both are observed as resting states under catalytic conditions for FA dehydrogenation. No further iridium species are observed in the catalytic reaction.

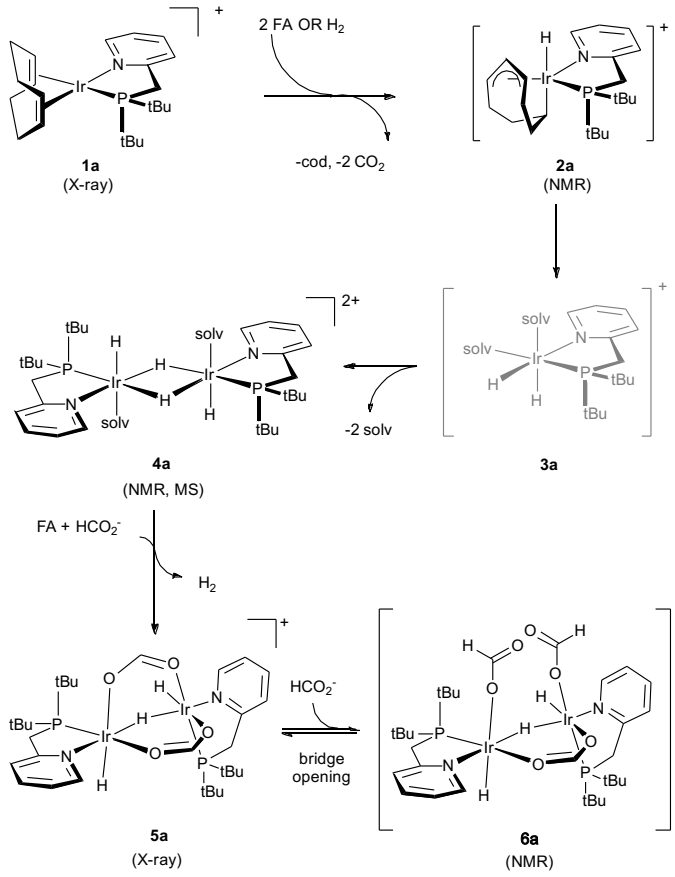


**Scheme 2.** A proposed catalyst initiation mechanism of iridium complex **1a**.

From kinetic evidence,[33] we concluded that the mechanism of catalytic formic acid dehydrogenation from **5a**/**6a** proceeds with rate-determining H-H bond formation followed by rapid decarboxylation to return **5a**. This work is explained elsewhere.[19,20] Further, we are stunned that, despite extensive investigation of highly analogous complexes over many years,[34] precatalyst **1a** was not identified for its reactivity with FA prior to our work. Thus, we set about to track the initiation of a family of complexes **1** to see if these convert to **4** or **5** under our FA dehydrogenation conditions and compare the results of these synthetic studies with reaction kinetics data for the dehydrogenation process.

### 2. Synthesis and characterization of Ir(COD) precatalysts

A general synthetic method was developed for iridium complexes **1a**-**1i**. They can be prepared by adding slowly the appropriate bidentate ligand to a dichloromethane solution of $[Ir(COD)Cl]_2$ (Scheme 3). After stirring at room temperature for 2 hours, insoluble salts were filtered off and the reaction mixture was treated with hexanes to yield the corresponding products as yellow to pale red powders. The structures of the products were confirmed by spectral and crystallographic data. As expected, crystal structures of **1a**, **1h**, and **1i** show that these complexes adopt the structure with a square planar iridium center.[16,20,21]

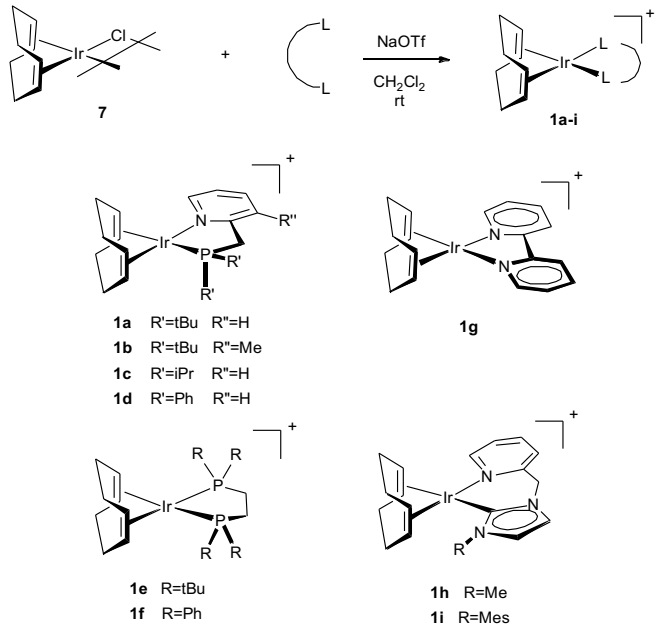


**Scheme 3**. Synthesis of iridium complexes **1a**-**1i**. Reaction time is 2 hours.

### 3. Conversion of mononuclear precursors to binuclear complexes

Knowing that C2-symmetrical iridium dimer **5a** is a catalytic resting state in FA dehydrogenation, we determined to evaluate whether structures analogous to **5a** are available to other iridium complexes shown in scheme 3. To do so we developed mild, stepwise conditions that simulate catalytic initiation, in which we observe clean conversion of **1a** to **4a'** and **5a'**, as monitored by proton NMR (Scheme 4). For this reaction, we chose acetic acid over formic acid, because the corresponding acetate complexes are resistant to dehydrogenation, thus promoting the stability of our target iridium intermediates.

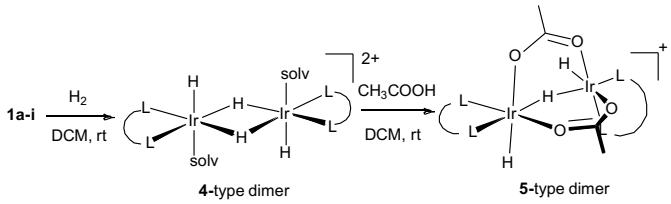


**Scheme 4**. Attempted conversion of iridium complex **1a-i** to **4**-type and **5**-type dimers. Conditions: 10 mg iridium complex **1**, 10 eq. acetic acid, ambient temperature, 1 h.

We used NMR and MS to monitor the conversion of iridium chelates **1bcdegh** under the conditions of scheme 4. Much to our surprise, despite the close structural homology of **1b-i** with **1a**, products found upon treatment with the conditions described in scheme 4 do not conform to the structure of **5**. In fact, only **1c**, **1d**, **1e,** and **1g** seem to have access to a **4**-type dimer, and even these reactions are not as selective as the reaction of **1a**.

Results for the conversion of iridium complexes **1** are varied and complex. The data are best summarized through the analysis of iridium hydride signals visible in their respective $^1$H NMR spectra (Figure 1). The first two lines of this figure show the iridium hydride signals that result from the conversion of **1a** to **4a'** and **5a'**, respectively. While a small fraction of **6a'** can be seen in the spectrum of **5a'**, the assignments of these spectra can be corroborated by comparison to their mass spectra and NMR data known for **4a** and **5a**.[20]

By remarkable contrast, complex **1b**, which differs from **1a** only by the addition of a methyl group in the complex's pyridine backbone, forms a complex mixture of products, none of which can be comfortably assigned as analogs of **4** or **5** according to NMR or MS. While it is possible that the aryl methyl group is perturbing the geometry of the catalyst's phosphinomethyl arm, we propose that this result shows that even a subtle perturbation of the electronics of the (pyridyl)phospine ligand of **1a** can disrupt its conversion to **4**/**5**. Complex **1c**, differing from the parent by only the deletion of a methyl from the phosphine *tert*-butyl group, shows high conversion to species **4c'**, but no evidence of any C2 twisting to a **5c'** structure. It appears therefore that steric bulk in the phosphine groups of **1a** is critical to enabling the C2 twist. Complex **1d**, which differs from the parent by the substitution of *tert*-butyl groups with phenyl groups, also shows high conversion to a **4d'** dimer, but no C2 twisting. This further supports the finding that the steric bulk in the phosphine groups of **1a** is needed for a clean conversion to dimer **5a'**.

We investigated complexes **1e** and **1g** that contain only the phosphine or pyridine moieties present in the parent **1a**. Complex **1e**, with two *tert*-butyl supported phosphine ligands converts to dimer **4e'** in appreciable amounts but does not participate in a C2 twist to the **5e'** dimer. Complex **1g**, with the bipyridine ligands, behaves similarly: it converts to a **4g'** structure but fails to twist. Furthermore, according to MALDI data, complex **4g'** converts back to the monomeric precatalyst **1g** as the major species in solution. With these studies in mind, the effects of both the specific pyridine and phosphine groups present in **1a** are needed cleanly to effect the C2 twist to a **5**-type structure.

We find that carbene-supported complex **1h** does not dimerize at all according to NMR and MS evidence. This is consistent with our observation of catalytic reactions involving **1h** in other catalytic reactions. For example, our processes for glycerol oxidation[16] and triglyceride upgrading[18] proceed through monomeric iridium complexes derived from **1h**. Our method for primary alcohols oxidation,[22] proceeds through a dimeric derivative of **1a** that is not related to **4** or **5**, and we suspect that 1h behaves like 1a in this reaction. These observations could help explain the complexity of the data shown for **1h** in figure 1, because we've shown that there are many productive pathways for initiation of **1h** and that none of them involve dimeric structures analogous to **4** or **5**.

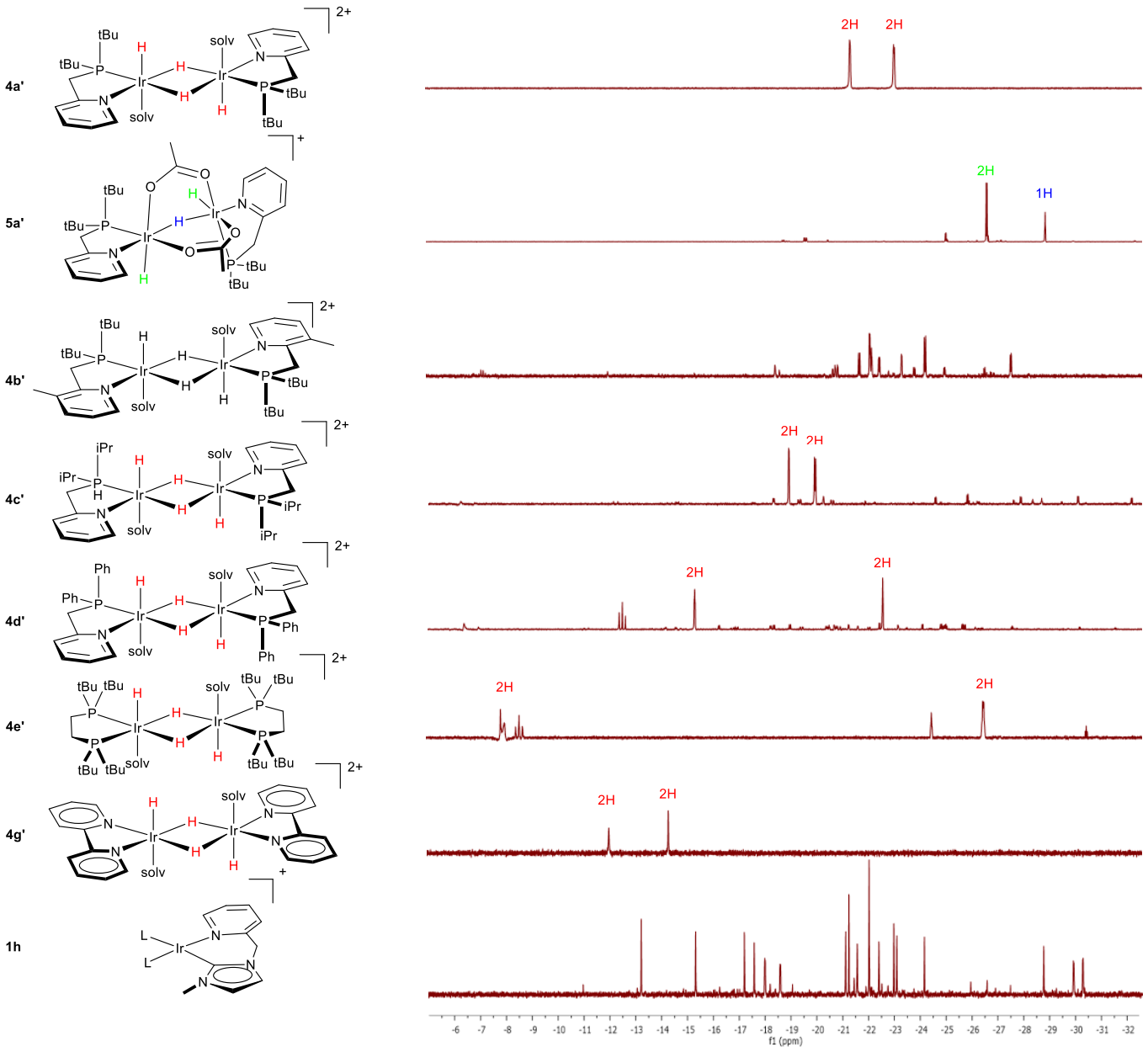


**Figure 1.** Results from treatment of various precursors with catalyst initiation conditions for formic acid dehydrogenation. Structures illustrated are predicted target structures, which were confirmed in some cases by identification of characteristic hydride signals. See supporting information for full $^{1}H$ spectra and, where available $^{31}P$ spectra. Also included are spectra for the conversion of **1a** to **4a'** upon exposure to hydrogen in acetonitrile.

#### 4. Catalytic FA dehydrogenation by iridium complexes

Even though **1b**-**1i** do not form a **5**-type dimer efficiently, some of them are catalysts for FA dehydrogenation under the same conditions that are optimized for **1a**. Kinetic data collected for FA dehydrogenation by iridium complexes **1** are striking (Figure 2). The reaction catalyzed by **1a** is much faster than any other, reaching completion in only 3 hours. By contrast, iridium complex **1c,** the most reactive of all of the derivatives studied, delivers less than 80% conversion after 24 hours. While **1b** and **1c** deliver some turnover of formic acid, all other complexes are unreactive compared to **1a**. The observation of an upward curvature of the kinetic profile of **1a** can be explained in that the decomposition of FA to gaseous $H_2$ and $CO_2$ reduces the volume of the solution and therefore increases the concentrations of both formate and the iridium catalyst.

The extraordinary reactivity of **1a** cannot simply be ascribed to electronic and/or steric effects. For example, complex **1a** has only two methyl groups more than **1c** and one fewer than **1b**. Poor reactivity of **1b** teaches us that there is most likely an

electronic effect in the C2 twist, and the performance of **1c** shows that sterics also are important.

We observe dramatic contrast between P—N supported **1a** and C—N supported **1h** and **1i**. *N*-Heterocyclic carbenes (NHCs) are often compared to phosphine ligands in coordination chemistry, as both are spectator ligands and strong sigma donors.[35,36] The "on" and "off" reactivity difference observed on the P—N and C—N motifs strongly suggests a reaction pathway available only to the P—N catalysts. We have previously proposed that this is because strongly-donating carbene ligands cause iridium hydride complexes to be high in energy and short-lived.[19]

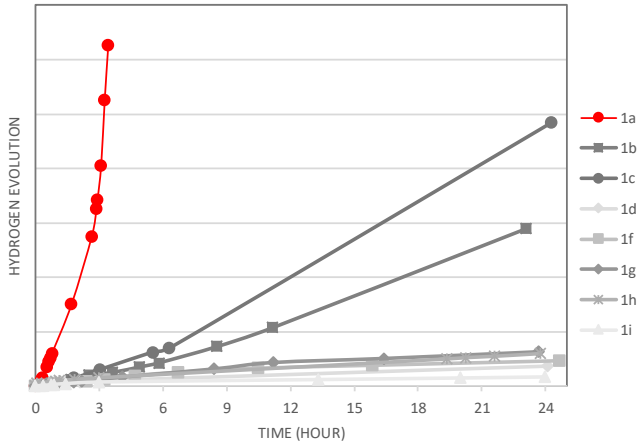


**Figure 2.** Catalytic dehydrogenation of neat FA monitored by eudiometer. Conditions: 90 °C, 1.0 mg NaOOCH, [Ir] = 15 μmol, 2.0 mL neat formic acid.

Figure 2 shows that iridium complex **1a** has a unique reactivity advantage over its analogues **1b-1i**. Connecting this observation to the structural observation that only **1a** converts cleanly to a C2-symmetric binuclear complex (**5a**) under catalytic conditions while **1b-1i** either stop the initiation sequence at the **4**-like dimer or turn into intractable mixtures of multiple species, we find that failure of **1b-1i** to enable efficient catalysis is related to a failure of the catalyst precursor to engage in the C2 twisting behavior observed in the conversion of **4a** to **5a**. We believe that the relationship is causal, i.e., that a successful C2 twist causes good catalytic performance.

## Conclusions

We show here that the formation of C2-symmetrical binuclear species **5a** is essential for the formation of the catalytically active species in neat formic acid dehydrogenation by **1a**. We propose that only iridium complexes in this series that can access **5**-type geometry have useful reactivity in dehydrogenation of neat FA. Kinetic data and structural analysis of an array of eight iridium complexes support this proposal. Future experiments on elucidation of the mechanism of FA dehydrogenation are under way.

## Experimental

### I. General Procedures

All air- and water-sensitive procedures were carried out either in a Vacuum Atmospheres glovebox under nitrogen (0.5–10 ppm of $O_2$ for all manipulations) or using standard Schlenk techniques under nitrogen. Deuterated NMR solvents were purchased from Cambridge Isotopes Laboratories. Benzene and dichloromethane-$d_2$ were dried over sodium benzophenone ketyl and distilled prior to use. Formic acid (HCOOH) was purchased from Sigma-Aldrich and used under a $N_2$ atmosphere without further purifications. Acetic acid was dried over $CaH_2$ and distilled prior to use. The integrity of this material was checked regularly by NMR. Cyclooctadiene iridium chloride dimer (**7**) was purchased from Sigma-Aldrich and used as received. Sonication procedures were done in a VWR desktop sonic cleaner bath. Silver trifluoromethylsulfonate was purchased from Alfa Aesar and used as received. $^{1}H$, $^{13}C$, and $^{31}P$ NMR spectra were obtained on Varian 600 or 500 MHz spectrometers with chemical shifts reported in units of ppm. All $^{1}H$ chemical shifts were referenced to the residual $^{1}H$ solvent (relative to TMS). NMR spectra were taken in 8-inch J-Young tubes (Wilmad) with Teflon valve plugs. All spectra were processed using MesRe Nova (v.11.0.4-11998). MALDI mass spectrometry was conducted on a Bruker Autoflex system.

### II. Preparative Details of Precatalysts 1

Iridium complex **1a**: complex **1a** was prepared in the drybox under nitrogen. 2-((Di-t-butylphosphino)methyl)pyridine[37] (105 mg, 0.440 mmol) was dissolved in a dry vial in 5 mL of dry dichloromethane. In another vial containing a Teflon stir bar, chloro(1,5-cyclooctadiene)iridium(I) dimer (149 mg, 0.220 mmol) and sodium triflate (130 mg, 0.750 mmol) were suspended in 10 mL of dry dichloromethane. The suspension was stirred vigorously and then the phosphinopyridine solution was added slowly dropwise. The phosphinopyridine vial was rinsed with 5 mL of dichloromethane and added to the stirred suspension. After stirring for 1 h, the solution was filtered to remove insoluble materials. The solvent was evaporated under reduced pressure to yield an orange, glassy solid. A 5:1 mixture of dry hexanes/ethyl ether (10 mL) was added to the residue, which was then triturated with the aid of sonication. The hexane was decanted and the residue washed with an additional 10 mL of hexanes/ethyl ether. The pure iridium complex **1a** was dried under reduced pressure to give an orange solid (235 mg, 77.3%).[20]

**1b-d:** Iridium complexes **1b-d** were prepared following the same method as **1a**. The pyridylphospine ligands for **1b** and **1c** were prepared similarly to literature methods as in **1a**. The pyridylphosphine ligand for **1d** was modified from known literature (see Supplementary Information).[38]

**1e-i:** Iridium complexes **1e-i** were prepared according to literature procedure.[16,39–41]

**III. Conversion of Precatalysts 1 to 4- and 5-type dimers**

**4**-Type species: In a typical reaction, iridium complex (5.0 mg) was placed in a J-Young NMR tube in a glovebox. Then, 0.60 mL of dried deuterated dichloromethane was placed in the tube and the tube was sealed. The complexes dissolved readily to form a red solution. The tube was then taken out of the glovebox and affixed to a Schlenk line. The tube was evacuated under reduced pressure, but only very briefly so as to prevent volatiles from escaping. The tube was then, while still on the Schlenk line, filled with $H_2$ gas. The tube was sealed and shaken until the red solution turned yellow, which happens rapidly upon mixing.

In the case of figure **1**, the isolation of complex **4a** was done by following this same method substituting acetonitrile for dichloromethane.

**5**-Type species: In a typical reaction, the J-Young NMR tube from the previous conversion to a **4**-type species was taken into a glovebox. Acetic acid (glacial, dry, 10 equivalents) were added to the tube solution via a microsyringe. The tube was then sealed and shaken and allowed to sit for 1 hour prior to NMR studies.

**IV. Hydrogen Quantification**

In a typical reaction, formic acid (2.0 mL, 53 mmol) and sodium formate (1.0 mg, 0.022 mmol) were combined with the analyte iridium complex **1** (15 µmol) in a 2 mL Schlenk bomb equipped with a Teflon stir bar while in a glovebox under nitrogen. A eudiometer was constructed as follows: the side arm of the valve of the Schlenk flask was connected to a piece of Tygon tubing, which was adapted to 20 gauge (0.03 inch) Teflon tubing with a needle. The tubing was threaded through an inverted 1 L graduated cylinder filled with water. The reactor's valve was opened to release gas from the reactor headspace while heating in a regulated oil bath. The volume of liberated gas was recorded periodically until gas evolution ceased. Liberated hydrogen was quantified by recording its volume displacement in the eudiometer.

## Conflicts of interest

There are no conflicts to declare.

## Acknowledgements

This work is sponsored by the NSF (CHE-1566167), and the Hydrocarbon Research Foundation. We thank the NSF (DBI-0821671, CHE-0840366, CHE-1048807) and the NIH (S10 RR25432) for analytical instrumentation. Fellowship assistance from the USC undergraduate research apprentice and provost fellowship programs (E. A. K., P. J. L.) is gratefully acknowledged. Support from the Jerome A. Sonosky fellowship of the USC Wrigley Institute (Z. L. and J. J. A. C.) is also appreciated.

## Notes and references

1 M. Grasemann and G. Laurenczy, *Energy Environ. Sci.*, 2012, **5**, 8171–8181.
2 F. Joó, *ChemSusChem*, 2008, **1**, 805–808.
3 A. Bulut, M. Yurderi, Y. Karatas, Z. Say, H. Kivrak, M. Kaya, M. Gulcan, E. Ozensoy and M. Zahmakiran, *ACS Catal.*, 2015, **5**, 6099–6110.
4 A. Beloqui Redondo, F. L. Morel, M. Ranocchiari and J. A. Van Bokhoven, *ACS Catal.*, 2015, **5**, 7099–7103.
5 S. Zhang, Ö. Metin, D. Su and S. Sun, *Angew. Chem. Int. Ed.*, 2013, **52**, 3681–3684.
6 M. Ojeda and E. Iglesia, *Angew. Chem. Int. Ed.*, 2009, **48**, 4800–4803.
7 J. Li, Q.-L. Zhu and Q. Xu, *Chimia (Aarau).*, 2015, **69**, 348–352.
8 M. D. Marcinkowski, J. Liu, C. J. Murphy, M. L. Liriano, N. A. Wasio, F. R. Lucci, M. Flytzani-Stephanopoulos and E. C. H. Sykes, *ACS Catal.*, 2017, **7**, 413–420.
9 T. C. Johnson, D. J. Morris, M. Wills, G. Laurenczy, J. R. Noyes, S. Gladiali, M. Beller and A. L. Spek, *Chem. Soc. Rev.*, 2010, **39**, 81–88.
10 E. A. Bielinski, P. O. Lagaditis, Y. Zhang, B. Q. Mercado, C. Würtele, W. H. Bernskoetter, N. Hazari and S. Schneider, *J. Am. Chem. Soc.*, 2014, **136**, 10234–10237.
11 C. Chauvier, A. Tlili, C. Das Neves Gomes, P. Thuéry and T. Cantat, *Chem. Sci.*, 2015, **6**, 2938–2942.
12 A. Boddien, D. Mellmann, F. Gartner, R. Jackstell, H. Junge, P. J. Dyson, G. Laurenczy, R. Ludwig and M. Beller, *Science*, 2011, **333**, 1733–1736.
13 J. F. Hull, Y. Himeda, W.-H. Wang, B. Hashiguchi, R. Periana, D. J. Szalda, J. T. Muckerman and E. Fujita, *Nat. Chem.*, 2012, **4**, 383–388.
14 Z. Lu, B. L. Conley and T. J. Williams, *Organometallics*, 2012, **31**, 6705–6714.
15 Z. Lu and T. J. Williams, *ACS Catal.*, 2016, **6**, 6670–6673.
16 Z. Lu, I. Demianets, R. Hamze, N. J. Terrile and T. J. Williams, *ACS Catal.*, 2016, **6**, 2014–2017.
17 X. Zhang, L. Kam, R. Trerise and T. J. Williams, *Acc. Chem. Res.*, 2017, 86–95.
18 Z. Lu, V. Cherepakhin, T. Kapenstein and T. J. Williams, *ACS Sustain. Chem. Eng.*, 2018, **6**, 5749–5753.
19 Z. Lu, V. Cherepakhin, I. Demianets, P. J. Lauridsen and T. J. Williams, *Chem. Commun.*, 2018, **54**, 7711–7724.
20 J. J. A. Celaje, Z. Lu, E. A. Kedzie, N. J. Terrile, J. N. Lo and T. J. Williams, *Nat. Commun.*, 2016, **7**, 11308.
21 Crystallographic data for compounds 1a (CCDC 1415049), 2a (CCDC 1815570), 5a' (CCDC 1415050), 1h (CCDC 1438247), and 1i (CCDC 1438246) can be obtained free of charge from The Cambridge Crystallographic Data Centre via www.ccdc.cam.ac.uk/data_request/cif.
22 V. Cherepakhin and T. J. Williams, *ACS Catal.*, 2018, **8**, 3754–3763.
23 S. Gruber, M. Neuburger and A. Pfaltz, *Organometallics*, 2013, **32**, 4702–4711.
24 S. Cohen, V. Borin, I. Schapiro, S. Musa, S. De-Botton, N. V. Belkova and D. Gelman, *ACS Catal.*, 2017, 8139–8146.

25 A. Matsunami, S. Kuwata and Y. Kayaki, *ACS Catal.*, 2017, **7**, 4479–4484.
26 M. Iguchi, H. Zhong, Y. Himeda and H. Kawanami, *Chem. - A Eur. J.*, 2017, **23**, 17017–17021.
27 Z. Hou, T. A. Koizumi, A. Fujita, H. Yamazaki and Y. Wakatsuki, *J. Am. Chem. Soc.*, 2001, 123, 5812–5813.
28 T. M. Gilbert and R. G. Bergman, *J. Am. Chem. Soc.*, 1985, **107**, 3502–3507.
29 Y. E. Begantsova, A. E. Varvarin, V. A. Ilichev and L. N. Bochkarev, *Russ. J. Gen. Chem.*, 2017, **87**, 1192–1197.
30 W. I. Dzik, S. E. Calvo, J. N. H. Reek, M. Lutz, M. A. Ciriano, C. Tejel, D. G. H. Hetterscheid and B. De Bruin, *Organometallics*, 2011, **30**, 372–374.
31 K. Ogata, T. Nagaya and S. I. Fukuzawa, *J. Organomet. Chem.*, 2010, **695**, 1675–1681.
32 E. S. Andreiadis, D. Imbert, J. Pécaut, A. Calborean, I. Ciofini, C. Adamo, R. Demadrille and M. Mazzanti, *Inorg. Chem.*, 2011, **50**, 8197–206.
33 Most striking in this study is the finding of half-order dependence on formate, which we rationalize by noting that in the conversion of **5a** to **6a**, one formate activates two sites on the catalyst. A free radical chain mechanism can also explain these kinetics, but we find no impact on rate with the addition of radical inhibitors such as BHT.
34 W.-H. Wang, Y. Himeda, J. T. Muckerman, G. F. Manbeck and E. Fujita, *Chem. Rev.*, 2015, **115**, 12936–12973.
35 S. P. Nolan, *N-Heterocyclic Carbenes in Synthesis*, 2006.
36 R. A. Moss and M. P. Doyle, *Contemporary Carbene Chemistry*, 2013.
37 C. Beddie, P. Wei and S. Douglas, *Can. J. Chem.*, 2006, **84**, 755–761.
38 R. Sun, H. Wang, J. Hu, J. Zhao and H. Zhang, *Org. Biomol. Chem.*, 2011, **12**, 5954–5963.
39 U. Hintermair, S. W. Sheehan, A. R. Parent, D. H. Ess, D. T. Richens, P. H. Vaccaro, G. W. Brudvig and R. H. Crabtree, *J. Am. Chem. Soc.*, 2013, **135**, 10837–10851.
40 M. Brill, D. Marrwitz, F. Rominger and P. Hofmann, *J. Organomet. Chem.*, 2015, **775**, 137–151.
41 W. A. Fordyce and G. A. Crosby, *Inorg. Chem.*, 1982, **21**, 1455–1461.

# Conformational Twisting of a Formate-Bridged Diiridium Complex Enables Catalytic Formic Acid Dehydrogenation

Paul J. Lauridsen, Zhiyao Lu, Jeff J. A. Celaje, Elyse A. Kedzie, Travis J. Williams*

Catalytic reactivity is switched on for formic acid dehydrogenation by a single precursor's unique ability to form a geometrically twisted dimer.